Theor Chim Acta (1992) 81: 201–222

Theoretica Chimica Acta

Intermediate neglect of differential overlap spectroscopic studies on lanthanide complexes

I. Spectroscopic parametrization and application to diatomic lanthanide oxides LnO (Ln = La, Ce, Gd, and Lu)

M. Kotzian[1], N. Rösch[1], and M. C. Zerner[2]

[1] Lehrstuhl für Theoretische Chemie, Technische Universität München, W-8046 Garching, Federal Republic of Germany

[2] Quantum Theory Project, University of Florida, Gainesville, FL 32611, USA

Received January 7, 1991/Accepted March 19, 1991

Summary. The Intermediate Nelgect of Differential Overlap model for spectroscopy has been extended to lanthanide complexes by including spin-orbit coupling. The method uses atomic spectroscopy and model Dirac–Fock calculations on the lanthanide atoms and ions to obtain ionization potentials, Slater–Condon factors and basis sets. The spin-orbit interaction strength, $\zeta(nl)$, is acquired from atomic spectroscopy, and only one-center terms are formally included. Calculation then proceeds using one open-shell operator for all seven f-orbitals initially assumed degenerate to generate starting non-relativistic molecular orbitals for the subsequent configuration-interaction and spin-orbit calculation.

Calculations are performed on the monoxides La, Ce, Gd, and Lu where there are ample experimental assignments. In general, the results are quite good, suggesting that the calculated energies, oscillator strengths and spin-orbit splittings can be used with success in assigning spectra, even in those cases where jj-coupling is of intermediate strength.

Key words: INDO method for lanthanides – Spin-orbit interaction – Electronic spectra – Lanthanide monoxides

1. Introduction

The chemistry of f-elements (lanthanides and actinides) has become the subject of attention in many areas [1–4]. In addition to the common use of f-elements as NMR shift reagents in stereochemical analysis [5], f-element compounds are of much interest in such general areas as coordination and organometallic chemistry, catalysis, solid state chemistry, and analytic chemistry. f-elements are commonly used, for example, in biology and medicine as contrast agents in NMR imaging (Gd^{3+}) or as radiotherapeutica (^{166}Ho) and in industry as colorants of glass and enamel (Nd_2O_3), as catalysts, oxidants (Ce), optical glasses (La_2O_3), in lasers ($Y_3Al_5O_{12}$:Nd^{3+}), color TV (Y_2O_2S:Eu^{3+}), X-ray intensifying screens (LaOBr:Tb^{3+}), and so on. Characterizing the physical and chemical properties of f-element compounds provides an enormous field for both applied and theoretical research. Spin-orbit effects in the lanthanides are, in

general, as large as ligand-field effects. For this reason conventional approaches to the bonding and spectroscopy of such compounds are often complex. Molecular electronic spectroscopy provides particularly detailed information on the electronic structure of such compounds, but only in the case of inorganic solids is a classification of the excited states really convincing [1–3].

Sufficiently complete and reliable experimental energy level diagrams are available for only a few lanthanide compounds. In the case of large and covalently bonded organometallic complexes (solution) spectra are rather unresolved and little is known about the electronic structure. Detailed theoretical treatment of lanthanide complexes is relatively rare. Examples include investigations of the electronic structure of lanthanide (Ln) and actinide (An) cyclooctatetraene sandwich complexes [6–8] and of divalent bis(cyclopentadienyl)lanthanide compounds [9, 10] using quasi-relativistic SCF-Xα scattered-wave calculations. Recent relativistic LCAO Hartree–Fock–Slater calculations on the ground state of various actinocenes $An(COT)_2$ [11] and Dirac–Slater DVM calculations on LnX_3 [12] and AnX_4 [13, 14] are further examples for the application of density functional methods to heavy element containing compounds. *Ab initio* pseudopotential methods were employed to study ground state properties of diatomic lanthanide monoxides, monofluorides, and monohydrides [15] as well as excited states of uranocene [16]. A few applications of semiempirical SCF methods to *f*-element compounds are known. Examples include studies of the electronic structure of LnF_3 [17], $Cp_2Lu(Cl)\cdot THF$ [18], or various lanthanide halides [19]. These investigations are all of the Intermediate Nelgect of Differential Overlap (INDO) type and do not include the important effects of spin-orbit coupling.

Here, we continue our work on the spectroscopic parametrization of the INDO model [20–22] to account for optical spectra of various rare earth containing compounds.

Most frequently used in assigning experimental spectra of transition metal complexes is the ligand field model. This method is often applied to ionic compounds such as monoxides LnO [23–25] and *f*-elements in crystalline matrices [26, 27], solution [28, 29] and sometimes to organometallic compounds such as tris(η^5-cyclopentadienyl)praseodymium(III) and neodymium(III) derivatives [30, 31]. The intensities of electronic absorptions are calculated using fitted parameters from the experimental spectra [29, 32]. Ligand field calculations may often be viewed as a parametrization of experimental spectra. We wish to overcome this limitation with a suitable parametrized electronic structure method that will allow the prediction of the optical spectra for a broad variety of molecules.

The INDO model has proved a useful tool in calculating ground state properties of various types of molecules such as organic compounds [33], transition metal complexes [34], and lanthanide containing molecules [19]. Its spectroscopic modification INDO/S has been applied successfully to the spectroscopy of organic molecules [20, 21] and to a variety of transition metal compounds [22, 35]. After augmenting the INDO/S-CI procedure by a treatment of the spin-orbit interaction [36] we report here on the extension of the method to excited states of lanthanide molecules. A parametrization of the model is developed to yield a rather satisfactory representation of electronic spectra, requiring only a moderate computational effort. This method, which in its simplest form consists of a molecular orbital calculation followed by a singly excited configuration interaction (CIS) treatment, provides a procedure for investigating the electronic spectra of lanthanide compounds, as an alternative to ligand field theory (LFT), free of parameters based on individual complexes.

To derive and check a semiempirical parametrization of the INDO model adapted for spectroscopy we need experimental molecular spectroscopic data. Classes of molecules where well resolved spectra are available for this purpose are the hydrated trivalent ions and the lanthanide monoxides. In the former case the sharpness of the spectral bands is due to the fact that transitions result from $4f \rightarrow 4f$ excitations which are weakly influenced by environmental effects, a result of compactness of the $4f$ shell [28]. In the latter case laser-induced fluorescence spectroscopy (LIF) and optical-optical double resonance (OODR) is performed on gas phase LnO resulting in well resolved band systems [25, 37, 38]. Even so, it is difficult to assign Ω values to the bands and find enough links between band systems to assemble them in a comprehensive energy level diagram [25]. This was successfully done, for example, by Carette et al. for GdO [38] and by Dulick and Field for PrO [39], where in each case ligand field calculations were used to complete the assignments. For several lanthanide monoxide molecules more or less complete and interpreted spectra are available, as for example LaO [40, 41], CeO [37], PrO [39, 42], NdO [43], SmO [44], GdO [38, 45], TbO [46], DyO [47], HoO [48], YbO [49], and LuO [40]. Ligand-field calculations have been performed for nearly all these lanthanide monoxides [23, 24]. The detailed information provided both by experiment and, to some extent, by ligand field theory form the base information for the parametrization of the INDO/S model.

In this paper we first review the INDO method as developed for examining the electronic structure of lanthanide compounds. Basic approximations for the calculation of excited states including spin-orbit effects are then presented. The derivation of the spectroscopic parametrization for molecules based on the established parameters on both ends of the lanthanide transition series is demonstrated on the examples of LaO and LuO, and further checks on the reliability of this procedure are presented with the calculation of the spectra of GdO and CeO [50]. A study of the f^2 and f^{12} systems, PrO and TmO, has recently been completed [51]. We are currently examining the spectroscopy of the hydrated ions $Ln(H_2O)_x$ as further examples, with good initial progress. In doing this study, we confirm much of the ligand field findings for LnO (Ln = La, Ce, Pr, Gd, Tm, Lu) and provide more complete energy level diagrams as a basis for further experimental investigations.

2. Method

The Intermediate Neglect of Differential Overlap method, developed for examining the electronic structure of lanthanide compounds, is characterized by a basis set obtained from relativistic Dirac–Fock [52] atomic calculations, the inclusion of all one-center two-electron integrals, and a parameter set based on molecular geometry [19]. The salient features of the INDO model Hamiltonian including its parametrization will be summarized here.

The matrix elements of the Fock operator in the INDO approximation are given by:

$$F_{\mu\mu}^{AA} = U_{\mu\mu}^{AA} + \sum_{[\sigma,\lambda]\in A} P_{\sigma\lambda}[(\mu\mu \mid \sigma\lambda) - \tfrac{1}{2}(\mu\sigma \mid \mu\lambda)] + \sum_{\sigma\in B\neq A} P_{\sigma\sigma}(\bar{\mu}\bar{\mu} \mid \bar{\sigma}\bar{\sigma}) - \sum_{B\neq A} Z_B(\bar{\mu}\bar{\mu} \mid s^B s^B) \quad (1)$$

$$F_{\mu\nu}^{AA} = \sum_{[\sigma,\lambda] \in A} P_{\sigma\lambda}[(\mu\nu \mid \sigma\lambda) - \tfrac{1}{2}(\mu\sigma \mid \nu\lambda)] \quad \mu \neq \nu$$

$$F_{\mu\nu}^{AB} = \tfrac{1}{2}(\beta_A(\mu) + \beta_B(\nu))S_{\mu\nu} - \tfrac{1}{2}P_{\mu\nu}(\bar{\mu}\bar{\mu} \mid \bar{\nu}\bar{\nu}) \quad A \neq B$$

where

$$(\mu\nu \mid \sigma\lambda) = \int d\tau(1)\, d\tau(2)\chi_\mu^*(1)\chi_\nu(1)r_{12}^{-1}\chi_\sigma^*(2)\chi_\lambda(2). \tag{2}$$

$\boldsymbol{P}$ is the first order density matrix and is identical to the charge and bond order matrix in the orthonormal atomic orbital (AO) basis set. $F_{\mu\nu}^{AB}$ refers to a matrix element of the Fock operator $\langle \chi_\mu^A | \boldsymbol{F} | \chi_\nu^B \rangle$ with AO χ_μ^A centered on atom "A", $\boldsymbol{S}$ is the overlap matrix corresponding to these AO's. The expressions above are given for the closed-shell case for simplicity. In this way, no generality is lost concerning the discussion of the parametrization. The basis set, the determination of the atomic core integrals $U_{\mu\mu}$ from experimental atomic spectroscopy, and details concerning the two-electron integrals are described in Ref. [19]. In the spectroscopic version of the INDO method one-center two-electron integrals F^0 are chosen from the Pariser approximation [53] $F^0(\mu\mu) = IP_\mu - EA_\mu$, (IP = Ionization Potential, EA = Electron Affinity), and the two-center two-electron integrals are calculated using the Mataga–Nishimoto formula [54]:

$$\gamma_{\mu\nu} = \frac{1.2}{R_{AB} + 2.4/(\gamma_{\mu\mu} + \gamma_{\nu\nu})} \tag{3}$$

in which $\gamma_{\mu\mu} = F^0(\mu\mu)$ are the Slater–Condon integrals. This semiempirical parametrization has yielded a good reproduction of spectra of organic molecules [20, 21] and transition metal complexes [22, 35, 36] and is in rather wide use today. For the lanthanides the values for $F^0(ss)$, $F^0(dd)$, and $F^0(ff)$ were derived from tables of Brewer [55, 56] and Martin, Zalubas and Hagan [57] when they provide enough information. Since experimental values of F^0 could not be obtained for many elements by this fashion, relativistic Dirac–Fock calculations on all neutral and singly positive charged lanthanide atoms in the configurations $4f^{N-1}6p6s^2$, $4f^{N-1}5d6s^2$, and $4f^N6s^2$ were performed. With these calculations we were able to reproduce the variation of Slater–Condon integrals with atomic number in good agreement with the corresponding change of the available experimental ones and therefore derived a recipe to obtain all integrals from calculated Slater–Condon parameters. This procedure ensures that trends over the lanthanide series are included that otherwise would not have been accounted for in the case of a linear interpolation. We chose the configuration $4f^{N-1}5d6s^2$ of the neutral atoms and determined common factors between experimental and calculated Slater–Condon integrals over the whole lanthanide period. The derived values are 1.04, 0.80, and 0.55 for γ_{ss}, γ_{dd}, and γ_{ff}, respectively.

In the case of first-row transition metals, γ_{sd} was determined applying the formula for the average energy of a configuration [19] of an atom or ion [58]. This procedure does not yield a unique value for γ_{sd}, γ_{sf}, and γ_{df} in the case of lanthanide atoms. An attempt to determine these integrals by $\gamma_{\mu\nu} = \sqrt{\gamma_{\mu\mu}\gamma_{\nu\nu}}$ did not result in reasonable spectra. As a consequence, these parameters were fixed comparing experiment with calculated atomic and molecular spectra obtained after studies with single excited configurations in a configuration interaction treatment. Calculations were performed on several neutral and double charged atoms (La, Ce, Pr, Yb, Lu) and on molecules such as LnO, $Ln(H_2O)_9$ (Ce, Pr,

Table 1. Atomic Slater–Condon and spin-orbit parameters in the INDO/S-CI method ($F^0(\mu\mu)$ in eV and $\zeta(nl)$ in cm^{-1})

	La	Ce	Pr	Nd	Pm	Sm	Eu	Gd	Tb	Dy	Ho	Er	Tm	Yb	Lu
$F^0(ss)$	5.42	5.50	5.59	5.66	5.74	5.82	5.89	5.97	6.05	6.13	6.21	6.28	6.36	6.44	6.52
$F^0(dd)$	6.91	7.07	7.21	7.33	7.44	7.53	7.62	7.64	7.65	7.64	7.63	7.60	7.57	7.52	7.46
$F^0(ff)$	12.68	13.34	14.00	14.61	15.19	15.74	16.27	16.59	17.09	17.58	18.06	18.53	18.99	19.44	19.89
$F^0(sd)$	5.52	5.61	5.70	5.78	5.86	5.93	6.01	6.07	6.14	6.20	6.26	6.32	6.38	6.43	6.48
$F^0(sf)$	5.41	5.49	5.58	5.67	5.75	5.83	5.91	6.00	6.08	6.17	6.26	6.35	6.44	6.53	6.63
$F^0(df)$	8.67	8.89	9.10	9.29	9.46	9.61	9.75	9.81	9.86	9.90	9.92	9.94	9.94	9.92	9.89
$\zeta(4f)$	503	621	741	865	997	1142	1300	1456	1629	1817	2018	2234	2463	2719	2990

Nd, Tm) and $Ln(H_2O)_8$ (Nd, Tm). Again we found common factors to determine the Slater–Condon integrals for the other rare earth elements. These factors are 0.90, 0.80, and 0.78 for γ_{sd}, γ_{sf}, and γ_{df}, respectively. Slater–Condon integrals for the whole series are listed in Table 1.

Another set of parameters for which new values have to be assigned in the spectroscopic parametrization are the bonding parameters β that are purely empirical. These parameters might be expected to be distance and charge (oxidation state) dependent [36, 59]. In the case of lanthanide compounds three different parameters were introduced [19], $\beta_s = \beta_p$, β_d, and β_f. Analogous to the case of first-row transition metals [58] the value of β_s was fixed to -1 eV, whereas for β_f values between -12 eV (Ce) and -96 eV (Lu) are recommended for the calculation of diatomic lanthanide monoxides. Especially β_d was allowed a greater variability to account for periodic bond effects since the $5d$ orbitals form the major contributions to bonding. We used values of -12 eV (LaO, CeO, GdO, LuO) and -6 eV (PrO, TmO).

All SCF calculations were performed employing a generalized restricted open-shell Fock operator as described by Edwards and Zerner [60]. In the cases of LaO and LuO with one open $6s$ shell we use the coupling coefficients given in Table 1 of Ref. [60]. In all other cases we need two open shells due to the ground state configuration $4f^N6s$ rationalized below. New formulas were derived for the coupling coefficients $a^{\mu\nu}$ and $b^{\mu\nu}$ [60] depending on the $4f$ occupation number N:

$\alpha^{\mu\nu} =$	$b^{\mu\nu} =$	
$\left(\frac{7}{6N}(N-1), 1, 0\right)$	$\left(\frac{7}{3N}(N-1), 2, 0\right)$	$N = 1, \ldots, 7$
$\left(\frac{7}{6N^2}(14 + N(N-3)), 1, 0\right)$	$\left(\frac{7}{3N^2}(98 + N(N-15)), -2, 0\right)$	$N = 8, \ldots, 14$

To set up the CI Hamiltonian spinless one- and two-center integrals are obtained as described in Ref. [22]. For the generation of the matrix elements of the spin-orbit operator $H_{SO} = \xi(r)\boldsymbol{l} \cdot \boldsymbol{s}$ additional integrals are needed. For this, we limit ourselves to the inclusion of one-center integrals since this is the main contribution, as discussed in Ref. [36]. The angular part of the spin-orbit integrals involving the operators $\hat{l}_x$, $\hat{l}_y$, and $\hat{l}_z$ may be calculated analytically in the basis of real spherical harmonics [61, 62]; they are stored explicitly within the program. The radial integrals $\zeta^A(nl)$ are taken from atomic spectroscopy [27, 63]. In this fashion we incorporate the most important part of the atomic two-electron contributions [36]. Since the spectroscopic derived integrals $\zeta^A(4f)$ differ, because they originate from different sources (atomic spectra, crystal spectra), we estimated these values from the given data in such a manner that they give good results for molecules with an effective metal charge between 0 and $+1$. Experimental values for the integrals $\zeta^A(5d)$ and $\zeta^A(6p)$ are rare. For example, in the case of Ce IV the values $\zeta^{Ce}(5d) = 995.6\ cm^{-1}$ and $\zeta^{Ce}(6p) = 3138.0\ cm^{-1}$ are given in Ref. [27]. The values used for $\zeta^A(4f)$ are listed in Table 1.

The CI Hamiltonian and spin-orbit matrix elements are calculated over Slater determinants [64]. By a linear combination of the determinants this matrix is adapted to double-group symmetry. To account for half-integral total angular momentum Bethe [65] introduced an extension of standard groups, the crystal double-groups [66]. The CI Hamiltonian matrix elements are generated within

this formalism [67]. Both the space and the spin part of a wavefunction may be adapted to transform according to an irreducible representation of a double-group. The present double-group program is based on the groups C'_{2v}, D'_2, and D'_{2h} and therefore limited to molecules with at least two mirror planes perpendicular to each other. For integral total angular momentum the double-group irreducible representations are the standard ones, and are all one-dimensional. For half-integral J one two-dimensional irreducible representation is added to form the double-group. For an odd number of electrons the double-group adapted functions are single Slater determinants, whereas for an even number of electrons these functions are a linear combination of two Slater determinants with all spins opposite. The adaption to the double-groups C'_{2v}, D'_2, and D'_{2h} has the important advantage that the integrals of $\hat{l}_x\hat{s}_x$ and $\hat{l}_z\hat{s}_z$, are purely imaginary, and those of $\hat{l}_y\hat{s}_y$ are purely real [67]. Since the Cartesian components of the angular momentum operators each transform according to different one-dimensional irreducible representations, matrix elements of the spin-orbit operator between the symmetry-adapted functions contain at most one non-zero contribution, either $\hat{l}_x\hat{s}_x$, $\hat{l}_y\hat{s}_y$ or $\hat{l}_z\hat{s}_z$. Thus the matrix elements are either purely real or purely imaginary. If one takes care of the phase factor ($\pm i$, ± 1) by explicit bookkeeping, then one is left with a real symmetric Hamiltonian matrix instead of a complex hermitian matrix [67]. Diagonalization of the CI Hamiltonian matrix yields a real coefficient matrix, but requires the reintroduction of the phase factors.

In the CI calculations we consider only single substituted determinants relative to the ground state configuration (CIS) where the different molecular orbitals σ, π, δ, and ϕ arising from the atomic $4f$ orbitals are treated as one unity. This means that, for example, the substitution $\pi^2(f^2) \rightarrow \delta\phi(f^2)$ is considered to be of order zero. Furthermore, we tried to include as many low-lying metal configurations as possible. Charge-transfer excitations were excluded from the CI since they are high-lying and do not influence the low-lying excited states discussed here. We included all determinants with multiplicities up to that where all metal electrons are arranged to give the highest spin multiplicity. In the case of GdO with a ground state configuration $4f^7 6s$ the highest multiplicity is a nonet. Further constraints on the selection of configurations are rationalized below when we consider each molecule separately.

Transition probabilities are calculated taking into account only one-center contributions from the electric dipole operator. Matrix elements are calculated over the three Cartesian components of the dipole length operator in the basis of atomic orbitals and then transformed to the molecular orbital basis. These effective one-electron matrix elements are treated in the same manner as the one-electron Fock matrix elements in the double-group configuration interaction formalism. In this case, however, the calculation of matrix elements between different irreducible representations of the double-group are required. The Cartesian components $k = x, y, z$ of the transition moment for a transition from state I to J is then given by the relation:

$$\mu^k_{IJ} = \boldsymbol{c}_I^\dagger \boldsymbol{M}^k \boldsymbol{c}_J + N^k \delta_{IJ}$$

where $\boldsymbol{M}^k$ is one Cartesian component of the electric dipole matrix in the basis of double-group adapted determinants. $\boldsymbol{c}_I$ and $\boldsymbol{c}_J$ are the complex coefficient vectors of the states I and J, respectively, and N^k is the contribution from the nuclear framework, which is zero for $I \neq J$. The oscillator strength [68]

$$f = 4.7092 \times 10^{-7}[|\mu^x_{IJ}|^2 + |\mu^y_{IJ}|^2 + |\mu^z_{IJ}|^2]\, \Delta E_{IJ}$$

(ΔE_{IJ} in cm^{-1} and μ_{IJ} in Debye) can be related to experimental quantities such as extinction coefficients and cross sections [36].

3. Results

3.1. General considerations

The large number of low-lying electronic states and the strong spin-orbit interaction that occurs in the lanthanide oxides renders the interpretation of experiments and the construction of a suitably parametrized ligand field model quite difficult [25]. The spectra of LaO and LuO are by far the simplest since only doublet states lie in the energy region of interest and these can be described applying the Russell–Saunders coupling scheme [40]. Little is known about the electronic structure of GdO. The ground state is supposed to be a $^9\Sigma^-$ and several other nonet and septet states of Σ and Π symmetry follow at higher energy [38, 45]. CeO with one electron in the $4f$ shell has been the subject of intense spectroscopic studies [37]. The complete energy level diagram for the low-lying states could be assembled and these states could be correlated to the jj-coupled levels of the free Ce III atomic $4f6s$ configuration [37]. A similar correlation of the low-lying states of PrO with the ^2H and ^4H states of the Pr III atomic $4f^26s$ configuration was done by Dulick and Field [25, 39]. In all situations in which large spin-orbit effects entail Hund's case (c) basis functions $|J\Omega\rangle$ less knowledge is provided on the nature of the wavefunction than the more insightful case (a) functions $|J\Omega\Lambda S\Sigma\rangle$. We will base our interpretation on that of Field [25] where explicit coupling of the f-electron part is considered. In so doing we gain a better understanding of the spectra of the lanthanide monoxides [51]. Most spectroscopic work to date suggests that the jj-coupling scheme is more appropriate since the $4f$-$6s$ exchange integral G^3 is small compared to the spin-orbit splitting. This is not the case for first-row transition metal oxides where the electronic states can easily be characterized for nearly all cases by the Russell–Saunders LS coupling scheme as reviewed by Merer [69]. In these compounds the corresponding $3d$-$4s$ exchange integrals are comparable in magnitude to the spin-orbit splitting constant. Field [25] also predicted the ground state configuration and low-lying excited states of diatomic lanthanide oxides based on a LFT analysis and on experimental hyperfine splittings of low-lying states of PrO. The bonding situation, and hence the ground state properties, of the various rare earth monoxides are very similar within the series since the compact $4f$ shell does not contribute to the bond as will be shown in the subsequent section. In contrast, the spectroscopy is determined by the increasingly filled $4f$ shell. The energetically low-lying states can be approximately interpreted arising from the $4f^N6s$ configuration of the Ln^{2+} free ion perturbed by the ligand field.

3.2. Ground state

The INDO/S-CI calculations were performed using the experimental bond distances. These are 1.826 Å (LaO [70]), 1.820 Å (CeO [37]), 1.803 Å (PrO [71]), 1.812 Å (GdO [45]), and 1.793 Å (LuO [72]). In the case of TmO the bond distance was estimated at 1.795 Å using the values for HoO (1.799 Å [48, 73])

and LuO. We employed the restricted open-shell formalism at the SCF level [60]. Several calculations on LnO (Ln = La – Lu) molecules were undertaken with various metal configurations to find the ground state. Subsequent CI calculations on the basis of single-excited determinants confirmed the SCF result of a $4f^N6s$ ground state configuration for the molecules mentioned here.

The bonding in LnO contains both ionic and covalent contributions. The ionic component arises from the configuration $Ln^{2+}(4f^N6s^1)$ $O^{2-}(2s^2 2p_\sigma{}^2 2p_\pi{}^4)$, where the $4f$ orbital occupation N is zero for lanthanum and increases with the atomic number. Exceptional cases are EuO and YbO with an experimental ground state configuration of $4f^{N+1}4f^{N+1}$ [25]. The covalent part of the bonding is best explained by starting with the pure ionic case, $Ln^{2+}O^{2-}$. The covalent interaction connects the O $2s$, $2p$ and Ln $5d$ orbitals. Contributions from Ln $6s$, $6p$, and $4f$ orbitals are negligible and only seem to polarize the $5d$ orbitals. In the present calculation bonding and charge transfer between O^{2-} and Ln^{2+} is much stronger in the $2p_\pi$-$5d_\pi$ interaction than it is in the $2s$-$5d_\sigma$ and $2p_\sigma$-$5d_\sigma$ interactions. As a typical example the ground state wavefunction of CeO is given in Table 2. For this molecule the total metal contribution to the π bond is 23% (22% $5d$), to the 1σ is 13% (7% $5d$), and to the 2σ is 16% (9% $5d$). This mixing results in the formal transfer of 0.91 electrons from O^{2-} into the metal π orbitals and 0.33 electrons into the σ orbitals reducing the charge on the Ce atom from 2 to +0.76. Note that the f orbitals for this case contain nearly 1.0 electrons as a result of the fact that they, by-and-large, do not contribute to the covalent bonding (see below).

This dominance of the π type interaction may be rationalized by the spatial extension of the various orbitals as exhibited by their radial expectation values (for Ce II): $\langle 6s \rangle = 2.22$ Å and $\langle 6p \rangle = 2.53$ Å. These values should be compared

Table 2. ROHF ground state wavefunction of CeO. – Orbital energies are given in eV. The numbering of the different irreducible representations starts with the valence orbitals. In the ROHF procedure one electron is assigned to the $4f$ shell resulting in fractional occupations as given in column "Occ.". Only atomic orbital contributions to the wavefunction with a coefficient exceeding 0.1 are displayed

Energy	MO	Occ.	Composition of wave function
−34.36	1σ	2	0.93 O2s + 0.28 Ce5d_σ + 0.19 Ce6p_σ + 0.15 Ce6s
−13.49	1π	4	0.87 O2p_π + 0.47 Ce5d_π + 0.12 Ce6p_π
−12.62	2σ	2	0.93 O2p_σ − 0.29 Ce5d_σ − 0.15 Ce4f_σ + 0.15 Ce6p_σ
−10.36	1ϕ	2/7	1.00 Ce4f_ϕ
−10.26	1δ	2/7	1.00 Ce4f$_\delta$
−10.16	2π	2/7	0.98 Ce4f_π
−10.05	3σ	1/7	0.97 Ce4f_σ − 0.23 Ce5d_σ
−6.30	4σ	1	0.95 Ce6s − 0.24 Ce5d_σ − 0.20 Ce6p_σ
−5.24	2δ		1.00 Ce5d_δ
−3.95	3π		0.92 Ce6p_π − 0.37 Ce5d_π + 0.11 O2p_π
−3.26	5σ		0.80 Ce6p_σ − 0.50 Ce5d_σ − 0.30 O2p_σ
−1.94	4π		0.78 Ce5d_π − 0.48 O2p_π + 0.38 Ce6p_π + 0.15 Ce4f_π
+1.00	6σ		0.69 Ce5d_σ + 0.51 Ce6p_σ − 0.35 O2s + 0.27 Ce6s + 0.20 O2p_σ + 0.14 Ce4f_σ

to the short bond length of 1.82 Å [37]. Therefore the corresponding Ce σ orbitals also overlap with the antibonding lobe of the O $2p_\sigma$ orbital, resulting in a smaller net σ than π overlap. This situation is analogous to findings in a recent LCGTO-LDF cluster investigation of localized excitons in alkali halides where an "inverted" Na $3d$ splitting in the octahedral field of the Cl^- ions was rationalized in a similar fashion [74]. The Ce and O $2s$ orbitals exhibit a much larger overlap, but contribute only weakly to the bonding because of the large energy separation between O $2s$ and Ce valence orbitals.

As discussed above, it is mainly the $5d$ orbitals of the metal that are involved in the bonding. The $4f$ orbitals are found nearly pure in the corresponding molecular orbitals. The coefficients of the $4f_{z^3}(\sigma)$ and $4f_{xz^2}$, $4f_{yz^2}(\pi)$ orbitals vary from 0.95 to 0.97 and 0.97 to 1.0, respectively, and the $4f_{z(x^2-y^2)}$, $4f_{xyz}(\delta)$ and $4f_{x^3-3xy^2}$, $4f_{y^3-3yx^2}(\phi)$ orbitals are nearly or totally unmixed for symmetry reasons. The σ and π type metal orbitals mix because of the perturbation of the oxygen ligand. The coefficient of the $5d$ dominated π orbital varies with the different lanthanides between 0.72 and 0.82 and lies above 0.84 in the molecular orbital with greatest $5p_\pi$ contribution. The mixing of the $6p_z$ and $5d_{z^2}$ σ orbitals is similar to that of CeO displayed in Table 2 for all the lanthanide monoxides examined here.

The wavefunction of CeO (see Table 2) does not support Field's assumption of a 50-50 Ce $6s$-O $2p_\sigma$ mixture for the 2σ and $3\sigma^*$ orbitals [25]. Nevertheless, the previous prediction of a $4f^N\sigma^*$ ground state for LnO ($4f^{N+1}$ for EuO and YbO) is confirmed in the present study, provided one formally replaces the σ and σ^* orbitals by two others, one orbital with predominant O $2p_\sigma$ and one with almost pure Ce $6s$ character. The low-lying electronic states of CeO may be interpreted assuming a $Ce(4f6s)^{2+}$ O^{2-} ground state configuration. The relative order of the various atomic configurations changes in CeO mainly due to the ligand field effect of O^{2-} [25]. The free ion ground state configuration of Ce III (Ce^{2+}) is $4f^2$ followed by $4f5d$ (lowest state: $^1G_4$, 3276.66 cm^{-1}), and $4f6s$ ($J = 2$, 19,236.23 cm^{-1}) [57]. To simulate ligand field effects model calculations were performed with a point charge X^{2-} at the place of the O^{2-} ligand. The ordering of the various Ce configurations changes to $4f6s < 4f^2$ (1200 cm^{-1}) $< 5d4f$ (9500 cm^{-1}) in $Ce^{2+}X^{2-}$ as compared to $4f6s < 5d\ 4f$ (6900 cm^{-1}) $< 4f^2$ (17,600 cm^{-1}) in CeO, indicative of a significant orbital influence beyond a simple LFT ansatz. The rearrangement of the configurations is affected by the different shielding behavior of $6s$, $6p$, $5d$, and $4f$ shells originating from their increasing radial extensions (in the order $4f < 5d < 6s < 6p$). LFT calculations predict the $4f^2$ and $5d4f$ configurations more than 30,000 cm^{-1} above the $4f6s$ manifold [25]. This seems to be in clear contradiction to experiment [37] where several unassigned states below 8000 cm^{-1} have yet to be accounted for.

A summary of the Mulliken population analysis is shown in Table 3. Compared to the pure ionic metal configuration $4f^N6s$ the metal accepts charge from O^{2-} through the σ and π orbitals. The formal occupation of the $6s$ orbital is reduced via the mixing with the $6p_\sigma$ and $5d_\sigma$ orbitals. The relatively high occupation of the $5d$ orbitals of about one electron characterizes the ground state occupation as $4f^N5d6s$. This averaged "configuration" based on the Mulliken population is not a good description of the ground state in a spectroscopic sense as will be discussed in the next sections. There is no formally occupied molecular orbital that is principally $5d$ in nature (see, for example, Table 2).

Table 3. Mulliken populations and atomic charge of selected lanthanide monoxides obtained from a ground state ROHF calculation. In orbitals of π, δ, and ϕ symmetry this is the sum of the populations of both orbitals

AO	LaO	CeO	PrO	GdO	TmO	LuO
O $2s$	1.922	1.923	1.945	1.950	1.958	1.949
O $2p_\sigma$	1.678	1.731	1.722	1.730	1.755	1.777
O $2p_\pi$	3.104	3.046	3.098	3.140	3.150	3.140
Ln $6s$	0.945	0.920	0.913	0.902	0.920	0.941
Ln $6p_\sigma$	0.135	0.079	0.087	0.065	0.054	0.038
Ln $6p_\pi$	0.012	0.029	0.037	0.053	0.061	0.049
Ln $5d_\sigma$	0.276	0.308	0.286	0.335	0.325	0.302
Ln $5d_\pi$	0.859	0.882	0.814	0.793	0.794	0.814
Ln $5d_\delta$	0.000	0.001	0.001	0.000	0.000	0.000
Ln $4f_\sigma$	0.044	0.181	0.335	1.018	1.707	1.994
Ln $4f_\pi$	0.026	0.329	0.623	2.015	3.425	3.997
Ln $4f_\delta$	0.000	0.284	0.570	2.000	3.429	4.000
Ln $4f_\phi$	0.000	0.286	0.571	2.000	3.429	4.000
Charge	0.704	0.700	0.765	0.819	0.858	0.866

3.3. *Configuration f^N, $N = 0, 7, 14$*

The ground state of LaO is $^2\Sigma^+$, of GdO $^9\Sigma^+$, and of LuO $^2\Sigma^+$. These three molecules are discussed together as they exhibit an empty, half-filled, and filled $4f$ shell, respectively, and therefore allow an examination of periodic trends. The energetic position of configurations differing by ± 1 $4f$ electron and the resulting influence on the spectrum will be discussed with each of the lanthanide monoxides. The lowest calculated charge transfer transition O → Ln from ligand to metal (LMCT) occurs from the O $2p_\sigma$ to the Ln $6s$ orbital. The lowest state arising from the resulting configuration $(2\sigma \mid 2p)^1(n\sigma \mid 6s)^1$ is found at energies of 51,600 cm^{-1} (LaO, $^2\Sigma^+$), 56,300 cm^{-1} (GdO, $^9\Sigma^+$), and 46,000 cm^{-1} (LuO, $^2\Sigma^+$), respectively. The first quartet states were calculated at energies of about 57,000 cm^{-1} (LaO: $2\sigma^1(3\sigma \mid 6s)^1(1\delta \mid 5d)^1$) and 58,400 cm^{-1} (LuO: $2\sigma^1(4\sigma \mid 6s)^1(2\delta \mid 5d)^1$).

LaO. The restricted open-shell ground state wave function can be approximately described as: $(1\sigma \mid \mathrm{O}2s)^2$ $(1\pi \mid \mathrm{O}2p)^4$ $(2\sigma \mid \mathrm{O}2p)^2$ $(3\sigma \mid \mathrm{La}6s)^2$ $(1\delta \mid \mathrm{La}5d)^0$ $(2\pi \mid \mathrm{La}6p)^0$ $(4\sigma \mid \mathrm{La}6p)^0$ $(3\pi \mid \mathrm{La}4f)^0$ $(1\phi \mid \mathrm{La}4f)^0$ $(5\sigma \mid \mathrm{La}4f)^0$ $(2\delta \mid \mathrm{La}4f)^0$ $(4\pi \mid \mathrm{La}5d)^0$ $(6\sigma \mid \mathrm{La}5d)^0$. The spectrum of LaO in the energy region of interest results only from the metal configurations $4f$, $5d$, $6p$, and $6s$. It is clear from atomic spectroscopy that excitations from inner shells do not fall into this energy region [57]. In the case of La III, no states resulting from a $5p^5$ configuration were observed and the $7s$ configuration is located at an energy of 82,347.26 cm^{-1} [57], in La IV the energy difference between the configurations $5p^6$ and $5p^54f$ is greater than 140,000 cm^{-1} [57].

Table 4 shows the calculated energy levels in comparison with experimental data [41]. Calculated and experimental electronic states were assigned taking into account selection rules and calculated transition moments. Experimentally

Table 4. Calculated and experimental [41] states of LaO. – State energies T_e are given in cm^{-1}. The molecular spin-orbit constant A is defined by the relation $\langle J\Omega\Lambda S\Sigma|H_{SO}|J\Omega\Lambda S\Sigma\rangle = A\Lambda\Sigma$

INDO/S-CI				Experiment		
State	Config.	T_e	A	State	T_e	A
$1^2\Sigma^+_{1/2}$	3σ 100%	0		$X^2\Sigma^+$	0	
$1^2\Delta_{3/2}$	1δ 100%	8488	353	$A'^2\Delta_r$	7468.9	350.5
$1^2\Delta_{5/2}$	1δ 100%	9195			8168.4	
$1^2\Pi_{1/2}$	2π 99%	13856	869	$A^2\Pi_r$	12635.7	862.7
$1^2\Pi_{3/2}$	2π 100%	14724			13497.6	
$2^2\Sigma^+_{1/2}$	4σ 93%	19715		$B^2\Sigma^+$	17837.8	
$2^2\Pi_{1/2}$	3π 94%	22986			22618.9	
$2^2\Pi_{3/2}$	3π 79% 2δ 20%	23241	255	$C^2\Pi_r$	22839.6	221.4
$1^2\Phi_{5/2}$	1ϕ 93%	23310	560			
$1^2\Phi_{7/2}$	1ϕ 100%	24990				
$2^2\Delta_{3/2}$	2δ 79% 3π 21%	24788	451			
$2^2\Delta_{5/2}$	2δ 93%	25691				
$3^2\Sigma^+_{1/2}$	5σ 90%	26007		$D(^2\Sigma)$	26959.0	
$3^2\Pi_{1/2}$	4π 99%	30180	408	$F(^2\Sigma)$	28049.0	
$3^2\Pi_{3/2}$	4π 99%	30588				
$4^2\Sigma^+_{1/2}$	6σ 100%	41616				

observed were the transitions labeled A ↔ X, B ↔ X, C ↔ X, D → X, and F → X [40]. This is consistent with the calculated transition moments given in Table 5. The $D^2\Sigma^+$ was assigned to the calculated $4f$ state $3^2\Sigma^+$ through its experimental vibrational constant ($\omega_e = 790\ cm^{-1}$ [40]) that is very similar to that of the $4f$ $2^2\Pi$ states (792.5, 798.4 cm^{-1} [40]). The $F^2\Sigma^+$ state can probably be assigned to the calculated state $3^2\Pi_{1/2}$. The next Σ state is calculated too high in energy for this association with F, even though its calculated energy lies above the experimental ionization potential (40,000 cm^{-1} [40]) and might be depressed by mixing with states in the continuum. On the basis of ligand field calculations including Rydberg-type orbitals Carette [41] assigned $D^2\Sigma^+$ and $F^2\Sigma^+$ to states mainly arising from the $7s$ and $8s$ configurations of the La^{2+} free ion, respectively. As our calculations do not contain orbitals that are $7s$ or $8s$ in nature we cannot confirm or deny this assignment, but based on spectroscopy of the ion we would expect such states to lie much higher in energy.

The splitting of the states $A'^2\Delta_r$ and $A^2\Pi_r$ was used to adjust the missing spin-orbit parameters $\zeta^{La}(6p) = 840\ cm^{-1}$ and $\zeta^{La}(5d) = 350\ cm^{-1}$. A strong mixture of the states $2^2\Pi_{3/2}$ and $2^2\Delta_{3/2}$ is observed. As a consequence, the molecular spin-orbit splitting constant A of the two states $2^2\Pi$ and $2^2\Delta$ is found very sensitive to changes in the parameter set. Two other experimentally observed transitions at energies of 14,671.19 and 15,150.00 cm^{-1} are assigned C → A′ [40] or possibly G → ? and E → ? according to [75]. We do not find a

Table 5. Calculated energies (in cm^{-1}) and oscillator strengths for the strongest transitions between states of LaO. The initial and final states are given in the first column and row, respectively. The energy difference is listed above the oscillator strength

$\|i\rangle\downarrow$ $\|f\rangle\rightarrow$	$1^2\Pi_{1/2}$	$1^2\Pi_{3/2}$	$2^2\Sigma^+_{1/2}$	$2^2\Pi_{1/2}$	$3^2\Sigma^+_{1/2}$	$3^2\Pi_{1/2}$	$3^2\Pi_{3/2}$
$1^2\Sigma^+_{1/2}$	13856 0.351	14724 0.373	19715 0.304	22986 0.021	26007 0.111	30180 0.007	30588 0.007
$1^2\Delta_{3/2}$	5368 0.008	6236 0.009					
$1^2\Delta_{5/2}$	4661 0.007	5530 0.008					
$1^2\Pi_{1/2}$						16324 0.0085	
$1^2\Pi_{3/2}$							15864 0.0073

reasonable transition in this energy region other than that between the components 1/2 and 3/2 of the states $1^2\Pi$ and $3^2\Pi$ with energy differences of 16,324 cm^{-1} and 15,864 cm^{-1}, respectively (see Table 5).

LuO. The ground state wave function of LuO can be approximated by: $(1\sigma \mid O2s)^2$ $(1\pi \mid Lu4f)^4$ $(1\phi \mid Lu4f)^4$ $(1\delta \mid Lu4f)^4$ $(2\sigma \mid Lu4f)^2$ $(2\pi \mid O2p)^4$ $(3\sigma \mid O2p)^2$ $(4\sigma \mid Lu6s)^1$ $(2\delta \mid Lu5d)^0$ $(3\pi \mid Lu6p)^0$ $(5\sigma \mid Lu6p)^0$ $(4\pi \mid Lu5d)^0$ $(6\sigma \mid Lu5d)^0$. The low-energy spectrum of LuO exhibits only states from the configurations 5*d*, 6*p*, and 6*s*. States arising from the subconfiguration $4f^{13}$ are expected at energies much higher than 100,000 cm^{-1}. The observed transitions in LuO are A→X, B→X, and C→X [40]. All assignments in Table 6 are done on the basis of transition probabilities and symmetry. The spin-orbit splitting of the state $1^2\Pi$ was again used to adjust the value for the atomic spin-orbit constant $\zeta^{Lu}(6p) = 2000\ cm^{-1}$. The value for $\zeta^{Lu}(5d)$ was estimated to 645 cm^{-1} from the calculated spectrum of LuF in a similar fashion.

GdO. The ground state wave function of GdO can approximately be described as: $(1\sigma \mid O2s)^2$ $(1\pi \mid O2p)^4$ $(2\sigma \mid O2p)^2$ $(1\phi \mid Gd4f)^2$ $(1\delta \mid Gd4f)^2$ $(2\pi \mid Gd4f)^2$ $(3\sigma \mid Gd4f)^1$ $(4\sigma \mid Gd6s)^1$ $(2\delta \mid Gd5d)^0$ $(3\pi \mid Gd6p)^0$ $(5\sigma \mid Gd6p)^0$ $(4\pi \mid Gd5d)^0$ $(6\sigma \mid Gd5d)^0$. The low-energy spectrum of GdO up to 26,000 cm^{-1} consists only of nonet and septet states arising from the configurations $4f^7 4\sigma$ ($1^9\Sigma^-$, $1^7\Sigma^-$), $4f^7 2\delta$ ($1^9\Delta$, $1^7\Delta$), $4f^7 3\pi$($1^9\Pi$, $1^7\Pi$), and $4f^7 5\sigma$ ($2^9\Sigma^-$, $2^7\Sigma^-$) (see Table 7). Only determinants of the $4f^7$ configuration are considered where each spin-orbital is occupied with one electron because all other $4f^7$ determinants are calculated at energies above 45,000 cm^{-1}. This restriction reduces the number of determinants for the configuration $4f^7 6s$ from 3432 to 256. States with lower multiplicity and those resulting from other configurations than presented in Table 7 are found at higher energies. The first septet states of the configuration $4f^8$, for example, are calculated above 47,000 cm^{-1}. Ligand field calculations [38] find a significant admixture of $4f^8$ (^7F) to the state $2^7\Sigma^-$ reversing the order of septet and nonet which is not confirmed by our calculations.

Table 6. Calculated and experimental [40] states of LuO. – State energies T_e are given in cm^{-1}. The molecular spin-orbit constant A is defined by the relation $\langle j\Omega\Lambda S\Sigma|H_{SO}|J\Omega\Lambda S\Sigma\rangle = A\Lambda\Sigma$. The oscillator strengths f are given for the transitions from the ground state

INDO/S-CI					Experiment		
State	Config.	T_e	A	f	State	T_e	A
$1^2\Sigma^+_{1/2}$	4σ 100%	0		—	$X^2\Sigma^+$	0	
$1^2\Delta_{3/2}$	2δ 100%	18486	639	$<10^{-4}$			
$1^2\Delta_{5/2}$	2δ 100%	19793		$<10^{-5}$			
$1^2\Pi_{1/2}$	3π 92%	23794	2135	0.300	$A^2\Pi_{1/2}$	(19392)	2078
$1^2\Pi_{3/2}$	3π 100%	25929		0.336	$B^2\Pi_{3/2}$	21470	
$2^2\Sigma^+_{1/2}$	5σ 93%	28424		0.178	$C^2\Sigma^+$	24440	
$2^2\Pi_{1/2}$	4π 100%	42695	752	0.053			
$2^2\Pi_{3/2}$	4π 100%	43447		0.064			

Table 7 displays the results of a CI calculation including the configurations mentioned above (1536 determinants) and compares them with experimental findings and a ligand field analysis [38]. The compositions of the molecular states are listed with the nonrelativistic states as reference. The latter states can be viewed equal to the molecular configurations since they are nearly unmixed. The ground state of GdO is $1^9\Sigma^-$ followed by $1^7\Sigma^-$. The calculated separation of these two states, about 1166 cm^{-1}, is small and that of the upper states $2^9\Sigma^-$ and $2^7\Sigma^-$ (of about 2500 cm^{-1}) large compared to the experimental values of 1840 cm^{-1} and 641 cm^{-1}, respectively [38]. The latter splitting decreases to about 1200 cm^{-1} when $4f^8$ configurations are included in the CI. The multiplet splitting in all Σ states is very small ($\approx$0.015 cm^{-1} in 1Σ) and consistent with experimental findings of $<10\ cm^{-1}$ [45]. The energies of the $2^{(7,9)}\Sigma$ states are too high compared to experiment [38], whereas the energetic positions of the $1^9\Pi$ and $1^7\Pi$ seem to be in excellent accord with experiment if the experimental assignment of $^9\Pi_4$ is correct [38]. Carette et al. [38] conclude on the basis of laser-induced fluorescence experiments that a significant mixing of $^9\Pi_4$ and $^7\Pi_4$ exists in this state which seems to confirm the assignment of our calculation (compare Table 7). The energy of the state $^9\Pi_1$ was calculated from the observed energy difference of 291 cm^{-1} between $^9\Pi_4$ and $^9\Pi_1$ [76]. No experimental energy levels of the Δ states are known. We relate this to the fact that the transition probabilities between the nearly unmixed Σ and Δ states ($\Delta\Lambda = 2$) are very small. We calculate the Δ manifold to lie lower in energy than does ligand field theory. Nevertheless, the $^9\Delta$ states should be energetically separated from the other states and therefore observable.

Table 7. Calculated and experimental [38] states of GdO. – State energies T_e are given in cm^{-1}. The composition of states is given in reference to the nonrelativistic states that most resemble the pure configurations. The ligand field energies are multiplet averaged values [38]

	INDO/S-CI		Experiment		LFT
Ω	T_e	Composition	State	T_e	T_e
	0	$1^9\Sigma^-$ 100%	$X^9\Sigma^-$	0	0
	1166	$1^7\Sigma^-$ 100%	$Y^7\Sigma^-$	1840	1999
2	8505	$1^9\Delta$ 100%			
1	8612	$1^9\Delta$ 99.7%			
0	8723	$1^9\Delta$ 99.5%			
1	8839	$1^9\Delta$ 99.3%			
2	8959	$1^9\Delta$ 99.2%			11594
3	9084	$1^9\Delta$ 99.2%			
4	9216	$1^9\Delta$ 99.3%			
5	9355	$1^9\Delta$ 99.5%			
6	9503	$1^9\Delta$ 100%			
5	14177	$1^7\Delta$ 99.4%			
4	14317	$1^7\Delta$ 99.2%			
3	14449	$1^7\Delta$ 99.1%			
2	14575	$1^7\Delta$ 99.1%			18188
1	14695	$1^7\Delta$ 99.3%			
0	14810	$1^7\Delta$ 99.5%			
1	14922	$1^7\Delta$ 99.7%			
3	17194	$1^9\Pi$ 96.1%			
2	17283	$1^9\Pi$ 89.5% $1^7\Pi$ 6.1%			
1	17372	$1^9\Pi$ 81.8% $1^7\Pi$ 12.8%			
0^-	17430	$1^9\Pi$ 74.5% $1^7\Pi$ 18.8%			
0^+	17562	$1^9\Pi$ 77.9% $1^7\Pi$ 18.9%			17647
1	17630	$1^9\Pi$ 69.4% $1^7\Pi$ 25.9%	$^9\Pi_1$	18181	
2	17750	$1^9\Pi$ 58.2% $1^7\Pi$ 35.8%			
3	17892	$1^9\Pi$ 45.0% $1^7\Pi$ 47.9%			
4	18060	$1^9\Pi$ 27.5% $1^7\Pi$ 64.2%	$A^9\Pi_4$	18472	
5	19846	$1^9\Pi$ 99.9%			
4	20092	$1^7\Pi$ 27.1% $1^9\Pi$ 71.9%			
3	20294	$1^7\Pi$ 44.5% $1^9\Pi$ 54.2%			
2	20471	$1^7\Pi$ 57.7% $1^9\Pi$ 41.0%			
1	20630	$1^7\Pi$ 68.5% $1^9\Pi$ 30.4%			19956
0^-	20767	$1^7\Pi$ 76.5% $1^9\Pi$ 22.3%			
0^+	20784	$1^7\Pi$ 79.3% $1^9\Pi$ 20.3%			
1	20910	$1^7\Pi$ 86.2% $1^9\Pi$ 13.3%			
2	21035	$1^7\Pi$ 93.5% $1^9\Pi$ 6.3%			
0^-	23507	$2^9\Sigma^-$ 92.1%			
1	23510	$2^9\Sigma^-$ 92.0%			
2	23519	$2^9\Sigma^-$ 91.8% $1^7\Pi$ 5.7%	$B^9\Sigma^-$	21647	26317
3	23533	$2^9\Sigma^-$ 91.3% $1^7\Pi$ 6.9%			
4	23554	$2^9\Sigma^-$ 90.8% $1^7\Pi$ 8.7%			
3	26039	$2^7\Sigma^-$ 96.8%			
2	26047	$2^7\Sigma^-$ 96.6%	$B_1{}^7\Sigma^-$	22261	25394
1	26051	$2^7\Sigma^-$ 96.4%			
0^+	26053	$2^7\Sigma^-$ 96.4%			

The level splittings in all Σ states are expected to be very small since there are no diagonal spin-orbit matrix elements ($l_z s_z$) between the multiplet components. Nonet and septet states with the same angular momentum Λ show the opposite splitting resulting in a continuous labelling by Ω when going from one multiplet component to the next. The separation of $^9\Delta$ and $^7\Delta$ is approximately the same as in the non-relativistic INDO/S-CI calculation (5500 cm^{-1}). The average splitting of the multiplet levels of both $^9\Delta$ and $^7\Delta$ is about 125 cm^{-1} (2A). This conforms to model considerations [63], where the molecular spin-orbit constant A is expected to be 1/8 of the atomic value (487 cm^{-1}). A slight increase of the multiplet splitting from 107 to 148 cm^{-1} is observed in going from the lowest spin component ($\Sigma = -4$) to the highest ($\Sigma = 4$). A qualitatively similar observation is found in the case of $^9\Pi$ and $^7\Pi$. The averaged multiplet splitting of 175 cm^{-1} (A) is about 1/8 of the corresponding $\zeta^{Gd}(6p) = 1486\ cm^{-1}$. As a consequence of the weaker electron repulsion, the nonet-septet separation (1800 cm^{-1}) is smaller and the interaction of both multiplets is stronger, resulting in a larger variation of the multiplet splittings. It is interesting to note that the contribution of $1^9\Pi$ decreases and of $1^7\Pi$ increases monotonously with energy within the two groups of Π levels ranging from 17,194 cm^{-1} to 18,060 cm^{-1} and from 20,092 cm^{-1} to 21,035 cm^{-1}, respectively.

Strong transitions with $\Delta\Omega = 0$ are found between the states of the same multiplicity of $1\Sigma^-$ and $2\Sigma^-$ symmetry with oscillator strengths of about 0.35 (nonet) and 0.39 (septet). Cross transitions between states of different multiplicities are weaker by a factor of about 50–100, but also observed spectroscopically [38]. The strongest transitions with $\Delta\Omega = \pm 1$ are calculated between $1^9\Sigma^-$ and $1^{(9,7)}\Pi$ and between $1^7\Sigma^-$ and $1^{(9,7)}\Pi$. Table 8 shows oscillator strengths between

Table 8. Oscillator strengths for the transitions between states $1^9\Sigma^-$ and $1^{(7,9)}\Pi$ of GdO. In the first column the energy difference between the Π multiplet levels and the $^9\Sigma$ levels are given. The multiplet levels of $^9\Sigma$ are nearly degenerate (see text). The oscillator strengths for the $\Delta\Omega = 0$ transitions are underlined

Energy	Λ_Ω	$^9\Sigma^-_{0^-}$	$^9\Sigma^-_1$	$^9\Sigma^-_2$	$^9\Sigma^-_3$	$^9\Sigma^-_4$
17194	Π_3				0.001	0.497
17283	Π_2		0.001	0.002	0.468	
17372	Π_1	0.005	0.004	0.452		
17430	Π_{0^-}	0.004	0.198			
17562	Π_{0^+}		0.203			
17630	Π_1	0.365	0.004	0.008		
17750	Π_2		0.314	0.005	0.001	
17892	Π_3			0.336	0.004	0.001
18060	Π_4				0.152	0.006
19846	Π_5					0.575
20092	Π_4				0.320	0.004
20294	Π_3			0.298	0.004	
20471	Π_2		0.234	0.004	0.022	
20630	Π_1	0.177	0.003	0.047		
20767	Π_{0^-}	0.002	0.042			
20784	Π_{0^+}		0.135			
20910	Π_1		0.001	0.042		
21035	Π_2			0.001		

the ground state $1^9\Sigma^-$ and the two Π multiplets. An overall decrease of oscillator strength is observed with increasing contribution of $1^7\Pi$ (compare Table 7) which is not astonishing since the initial states have nonet multiplicity. Since there is no detailed experimental characterization of electronic quantum numbers we are not able to assign the band system between 16,094 and 17,649 cm^{-1} given by Yadav et al. [45].

3.4. *Configuration f^1, CeO*

CeO has a very large number of states to be considered. One electron in the $4f$ shell results in 14 microstates. Therefore, one expects 28 or 140 determinants in the $4f6s$ or $4f5d$ configurations, respectively. The energy difference between the $4f6s$ ground state and the next configurations $4f5d$ and $4f^2$ is large enough for the $4f6s$ manifold to be only weakly disturbed by the higher-lying levels. Therefore a relatively instructive interpretation of the splittings in the $4f6s$ configuration can be given [50].

All states of the $4f6s$ configuration calculated from a CI including all Ce^{2+} valence configurations are shown in Table 9. Charge transfer excitations $O \rightarrow Ce$ ($> 55{,}000$ cm^{-1}) were omitted in the CI procedure. The experimental energies are reproduced very well by this calculation. For two pairs of states (U_1 0^+ and V_2 1; U_2 1 and U_3 0^+) the calculated order is reversed compared to experiment. In the first case, the ligand field model (LFT1) [23] and the INDO method agree. This

Table 9. Calculated and experimental states of CeO of the configuration $4f6s$. – Energies are given in cm^{-1}. In the first column the experimental labeling is given. Λ is the projection of the total orbital angular momentum, Ω the projection of the total angular momentum in the molecular system, and J_a the value of the atomic total angular momentum from which the molecular state originates. The values of Λ and J_a are taken from the leading determinant. Ligand field (LFT1, LFT2) and experimental values are taken from Refs. [23], [24], and [37], respectively

State	Λ	Ω	J_a	Exp.	LFT1	LFT2	INDO/S-CI		
							Energy	Configuration	
X_1	3	2	2	0.0	0.0	0	0	$1\phi4\sigma$ 91%	
X_2	3	3	3	80.3	121.6	197	71	$1\phi4\sigma$ 90%	
W_1	2	1	2	811.6	805.6	1026	857	$1\delta4\sigma$ 84%	
W_2	2	2	3	912.2	910.8	1160	918	$1\delta4\sigma$ 82%	$2\pi4\sigma$ 17%
V_1	1	0^-	2	1679.4	1777.7	1756	1812	$2\pi4\sigma$ 73%	$3\sigma4\sigma$ 25%
V_2	1	1	3	1869.7	1878.4	1919	1937	$2\pi4\sigma$ 70%	$3\sigma4\sigma$ 27%
U_1	1	0^+	3	1931.8	1866.3	1978	1850	$2\pi4\sigma$ 75%	$3\sigma4\sigma$ 22%
X_3	3	4	4	2039.8	2021.8	2495	2084	$1\phi4\sigma$ 99%	
X_4	3	3	3	2140.6	2185.4	2146	2154	$1\phi4\sigma$ 98%	
W_3	2	3	4	2617.3	2632.2	3268	2726	$1\delta4\sigma$ 84%	
W_4	2	2	3	2771.7	2762.7	2994	2791	$1\delta4\sigma$ 84%	
V_3	1	2	4	3462.6	3501.5	3944	3453	$2\pi4\sigma$ 80%	$1\delta4\sigma$ 17%
V_4	1	1	3	3642.0	3600.9	3724	3562	$2\pi4\sigma$ 81%	$1\delta4\sigma$ 14%
T_1	0	0^-	4	3821.5	4035.2	4109	4176	$3\sigma4\sigma$ 72%	$2\pi4\sigma$ 25%
U_2	0	1	4	4133.0	4101.9	4391	4234	$3\sigma4\sigma$ 68%	$2\pi4\sigma$ 29%
U_3	0	0^+	3	4457.7	4262.8	4476	4217	$3\sigma4\sigma$ 70%	$2\pi4\sigma$ 23%

order is affected by the exchange integral $G^3(sf)$ via the splitting of the states V_1 and V_2. The other pair of states may be influenced by low-lying states of the $4f5d$ configuration. The lowest states of $4f5d$ character are calculated at energies of 6564 cm^{-1} ($\Omega = 4$), 7876 cm^{-1} ($\Omega = 5$), and 8021 cm^{-1} ($\Omega = 0^+$), about 2500 cm^{-1} higher than expected from experiment [37].

The order of molecular states arising from the metal $4f6s$ configuration can be described from two different, but rather informative viewpoints. Figure 1 gives a schematic interpretation of the splittings in the lowest-lying molecular states of CeO. Starting with the non-relativistic atomic states ^1F and ^3F arising from the configuration $4f6s$ one can first "switch on" the spin-orbit interaction and then the ligand field or vice versa. Spin-orbit interaction causes the states ^1F and ^3F to interact according to the jj-coupling scheme resulting in four levels that are observed in atomic spectroscopy [57]. In going from Ce^{2+} (Ce III) to CeO in the "non-relativistic" case, the ligand field of O^{2-} causes the F ($L = 3$) states to split into the molecular states Φ, Δ, Π, and Σ ($\Lambda = 3, 2, 1, 0$). The z-component Λ in the molecular case, associated with atomic angular momentum L, decreases with increasing energy (compare Fig. 1). When the spin-orbit interaction is taken into account the pairs of states with the same value of Λ (e.g. $^1\Phi$, $^3\Phi$) split resulting again in the coupling pattern typical of Hund's case (c).

Coming from the left side of the figure, the atomic F states split under the influence of the ligand field to give a set of states where the atomic coupling pattern is retained in groups of levels whose z-component Ω of the total angular momentum J can be characterized by the atomic value J_a as we describe below. To summarize, the effect of the ligand field on the J states of CeO is similar to that found in the L states of molecules with lighter metal atoms, and the two perturbations, ligand field and spin-orbit interaction, seems to be additive. Table 9 displays in the first column the labelling according to the molecular system, e.g.

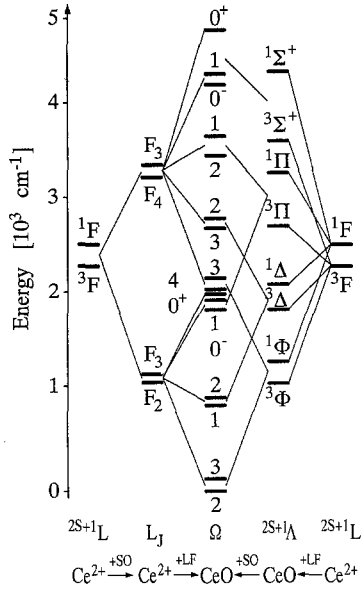

Fig. 1. Calculated states of Ce^{2+} and CeO

X_i result from $^1\Phi$ and $^3\Phi$. Furthermore, we list the total angular momentum quantum number J_a of the atomic parent state which, under the influence of the ligand field, yields the corresponding molecular level.

Grouping the levels according to $\Omega = J_a$ (X_i), $J_a - 1$ (W_i) and $J_a - 2$ (V_i) the typical case (c) pattern of the atomic states [57] is revealed (see above). The splitting caused by spin-orbit interaction decreases in steps of about 200 cm^{-1}. In a molecule (e.g. TiO) with small spin-orbit coupling where Λ and Σ are approximately good quantum numbers, a decrease in steps of ζ_{4f} (exp.: 640 cm^{-1} [63]) is expected. Another feature to be extracted from Table 9 is the effect of the ligand field. States with decreasing Ω (J_a fixed), e.g. X_1, W_1, and V_1 for $J_a = 2$, show that the ligand field of symmetry $C_{\infty v}$ repells the $4f$ orbitals in the order $\phi < \delta < \pi < \sigma$. We conclude that the ordering of the non-relativistic case, split by the ligand field and labelled according to Λ, is in keeping with that of the jj-coupled states characterized by the quantum number Ω. This is completely analogous to the findings for PrO and TmO [51].

4. Summary and conclusions

In our parametrization of the Intermediate Neglect of Diatomic Overlap model adapted for spectroscopy we have accounted for the three main interactions that determine the spectra of lanthanide complexes. First is the relative order of configurations which is determined mostly by the electrostatic interactions of the electrons on the metal center. This we accomplish in an accurate fashion by extracting parameters from atomic spectroscopy and from model Dirac–Fock calculations on atoms and ions. A second interaction, also predominantly one-center, concerns the multiplet splitting. Our choice of parametrizing the radial spin-orbit integrals $\zeta^A(nl)$ using data from atomic spectroscopy yields a rather good description of the multiplet splitting in molecules. Finally ligand field effects, both charge transfer and reduction in symmetry, appear to be well represented through an empirical choice of the resonance integral β, as well as the relative energies of core integrals calculated from experimental ionization potentials. This was not shown explicitly in this paper, but our calculations on CeO required a proper reproduction of these splittings in order to yield a good energy level diagram for the low-lying states. The adoption of atomic parameters $F^0(\mu\mu)$ from atomic spectroscopic data supplemented by relativistic Dirac–Fock calculations accounts for the nonlinear variation over the transition series. Slater–Condon parameters $F^0(\mu\nu)$ that were not accessible directly from spectroscopy were fixed at both ends of the period (La, Lu) and interpolated again using relativistic Dirac–Fock calculations as a guide and a simple scaling factor. The choice of parametrizing the spin-orbit constant $\zeta^A(nl)$ from atomic spectroscopy incorporates the two main contributions to spin-orbit splitting, the one-electron and two-electron one-center integrals.

In calculating the spectroscopy of the lanthanide compounds we start with a non-relativistic restricted open-shell calculation in which all the molecular $4f$ orbitals are considered degenerate and to lie in one open-shell since the ligand field splitting is shown to be small. The configuration-averaged restricted open-shell ground state Fock operator appears to generate a good basis for the succeeding configuration interaction procedure. The CI is performed using only single-substituted determinants relative to the ground state. Experience shows that inclusion of energetically higher-lying configurations generally results in

energy shifts of only a few wavenumbers. Although we can not yet generalize this simplification, the restriction to the principal configurations of interest reduces the computational effort considerably.

Since the electronic $4f$-$6s$ exchange integral G^3 is small compared to the atomic spin-orbit constant $\zeta^A(4f)$ in the cases of CeO, PrO, and TmO strong jj-coupling is observed. The total angular momentum J_f of the f-electron states which can be described by LS term symbols couples with the J_s of the s electron resulting in the typical Hund's case (c) pattern. These atomic states are split due to the molecular interaction according to Ω and this pattern is conserved in a "relativistic" treatment. Using these same approximations, Field [25] predicted the ground states of all lanthanide monoxides. The lowest-lying multiplet state ${}^{2S+1}L_J$ can be determined by Hund's rules in the atomic case. The J levels split according to $\Omega = J_a, J_a - 1, \ldots$ where $\Omega = J_a$ is the lowest state as shown here for the example of CeO [50], but this observation also holds for PrO and TmO [51]. Assuming a $4f^N6s$ ground state ($4f^{N+1}$ for EuO and YbO) the Ω values can be easily derived.

The order of energy levels with $\Omega = J_a, J_a - 1, \ldots$ has been shown to be qualitatively the same as that obtained from a non-relativistic treatment of states with labels $\Lambda = L_a, L_a - 1, \ldots, 0$. Where a large number of state arises from one configuration, higher-lying states may exhibit a strong mixing of states arising from different configurations. In these cases it is difficult to give a qualitative interpretation in terms of L and S since a small shift of a few hundred wavenumbers can result in a different interaction of the multiplet levels. Nevertheless, using predicted energies, oscillator strengths and spin-orbit splittings it should be possible to assign the observed spectra. This we have done here with some success for the lanthanide monoxides.

We have presented here a spectroscopic parametrization of the INDO model that extends its utility to lanthanide compounds, that includes spin-orbit effects and that accounts for the main features in the spectra of their oxides. Additionally, we have given new insight into the bonding of lanthanide monoxides and the understanding of the sequence of low-lying electronically excited states. We expect the set of parameters to be flexible enough for the treatment of the spectroscopy of organometallic rare earth compounds. In the past the parametrization of the first row transition metals has been shown to yield good results in the cases of ionic compounds [22] as well as more covalent organometallic molecules [35, 58], and we expect these findings to pertain to lanthanide compounds as well.

Acknowledgements. M. C. Zerner would like to acknowledge the great hospitality of Prof. G. H. F. Diercksen at the Max-Planck-Institut für Physik und Astrophysik (Garching) and that of the Technische Universität München where most of the work was done. This work was supported by the Deutsche Forschungsgemeinschaft, the Fond der Chemischen Industrie, and the Bund der Freunde der Technischen Universität München.

References

1. Croatto U (1984) 1st Int Conf Chem and Techn of the Lanthanides and Actinides (1st ICLA), Venice In: Inorg Chim Acta 94, 95
2. Croatto U, Bagnall KW, Marcalo J, Pires de Matos A (1987) 2nd Int Conf Basic and Applied Chemistry of f-Transition (Lanthanide and Actinide) and Related Elements (2nd ICLA), Lisbon In: Inorg Chim Acta 139, 140

3. Sinha SP (1983) Systematics and the properties of the lanthanides. Reidel, Dordrecht
4. Görller-Walrand C (1990) 1st Int Conf on *f*-Elements (1st ICFE), Leuven In: Eur J Solid State Inorg Chem 28.
5. Morrill TC (1987) Lanthanide shift reagents in stereochemical analysis. Verlag Chemie, Weinheim
6. Rösch N, Streitwieser A Jr (1983) J Am Chem Soc 105:7237
7. Rösch N (1984) Inorg Chim Acta 94:297
8. Streitwieser A Jr, Kinseley SA, Rigsbee JT, Fragala IL, Ciliberto E, Rösch N (1985) J Am Chem Soc 107:7786
9. Andersen RA, Boncella JM, Burns CJ, Green JC, Hohl D, Rösch N (1986) J Chem Soc Chem Comm :405
10. Green JC, Hohl D, Rösch N (1987) Organometallics 6:712
11. Boerrigter PM, Baerends EJ, Snijders JG (1988) Chem Phys 122:357
12. Ellis DE, Goodman GL (1984) Int J Quantum Chem 25:185
13. Ellis DE, Holland GF (1986) Chem Scripta 26:441
14. Hohl D, Ellis DE, Rösch N (1987) Inorg Chim Acta 127:195
15. Dolg M, Stoll H (1989) Theor Chim Acta 75:369
16. Chang AHH, Pitzer RM (1989) J Am Chem Soc 111:2500
17. Li LM, Ren JQ, Xu GX, Wang XZ (1983) Int J Quantum Chem 23:1305
18. Li J, Ren JQ, Xu GX, Qian CT (1986) Inorg Chim Acta 122:255
19. Culberson JC, Knappe P, Rösch N, Zerner MC (1987) Theor Chim Acta 71:21
20. Ridley JE, Zerner MC (1973) Theor Chim Acta 32:111
21. Ridley JE, Zerner MC (1976) Theor Chim Acta 42:223
22. Anderson WP, Edwards WD, Zerner MC (1986) Inorg Chem 25:2728
23. Dulick M, Murad E, Barrow RF (1986) J Chem Phys 85:385
24. Carette P, Hocquet A (1988) J Mol Spectrosc 131:301
25. Field RW (1982) Ber Bunsenges Phys Chem 86:771
26. Hüfner S (1983) Optical spectroscopy of lanthanides in crystalline matrix. In: Sinha SP (ed) Systematics and the properties of the lanthanides. Reidel, Dordrecht
27. Wybourne BG (1965) Spectroscopic properties of rare earths. Wiley, New York
28. Carnall WT (1979) The absorption and fluorescence spectra of rare earth ions in solution. In: Gschneidner KA, Eyring L (eds) Handbook on the Physics and Chemistry of Rare Earths, Vol 3 – Non-metallic compounds – I. North-Holland, Amsterdam
29. Carnall WT, Beitz JV, Crosswhite H, Rajnak K, Mann JB (1983) Spectroscopic properties of the *f*-elements in compounds and solution. In: Sinha SP (ed) Systematics and the Properties of the Lanthanides. Reidel, Dordrecht
30. Amberger HD, Schultze H, Edelstein NM (1985) Spectrochim Acta 41A:713
31. Amberger HD, Schultze H, Edelstein NM (1986) Spectrochim Acta 42A:512
32. Burdick GW, Downer MC, Sardar DK (1989) J Chem Phys 91:1511
33. Pople JA, Beveridge DL, Dobosh PA (1967) J Chem Phys 47:2026
34. Bacon AD, Zerner MC (1979) Theor Chim Acta 53:21
35. Kotzian M, Rösch N, Schröder H, Zerner MC (1989) J Am Chem Soc 111:7687
36. Kotzian M, Rösch N, Pitzer RM, Zerner MC (1989) Chem Phys Lett 160:168
37. Linton C, Dulick M, Field RW, Carette P, Leyland PC, Barrow RF (1983) J Mol Spectrosc 102:441
38. Carette P, Hocquet A, Douay M, Pinchemel B (1987) J Mol Spectrosc 124:243
39. Dulick M, Field RW (1985) J Mol Spectrosc 113:105
40. Huber KP, Herzberg G (1979) Molecular spectra and molecular structure, Vol IV. Constants of diatomic molecules. Van Nostrand, New York
41. Carette P (1990) J Mol Spectrosc 140:269
42. Shenyavskaya EA, Egorova IV, Lupanov VN (1973) J Mol Spectrosc 47:355
43. Kaledin LA, Shenyavskaya EA, Kovacs I (1983) Acta Phys Hungary 54:189
44. Linton C, Bujin G, Rana RS, Gray JA (1987) J Mol Spectrosc 126:370
45. Yadav BR, Rai SB, Rai DK (1981) J Mol Spectrosc 89:1
46. Gurvich LV, Dimitriev YN, Kaledin LA, Shenyavskaya EA (1984) Izvest Akad Nauk Ser Phys 48:721

47. Linton C, Gaudet DM, Schall H (1986) J Mol Spectrosc 115:58
48. Liu YC, Linton C, Schall H, Field RW (1984) J Mol Spectrosc 104:72
49. Linton C, McDonald S, Rice S, Dulick M, Liu YC, Field RW (1983) J Mol Spectrosc 101:332
50. Kotzian M, Rösch N (1991) Eur J Solid State Inorg Chem 28:127
51. Kotzian M, Rösch N (1991) J Mol Spectrosc 147:346
52. Desclaux JP (1975) Comp Phys Comm 9:31
53. Pariser R (1953) J Chem Phys 21:568
54. Mataga N, Nishimoto K (1957) Z Phys Chem 13:140
55. Brewer L (1971) J Opt Soc Am 61:1101
56. Brewer L (1971) J Opt Soc Am 61:1666
57. Martin WC, Zalubas R, Hagan L (1978) Atomic energy levels – the rare-earth elements. US Dept of Commerce, Natl Bureau of Standards, Washington
58. Zerner MC, Loew GH, Kirchner RF, Mueller-Westerhoff UT (1980) J Am Chem Soc 102:589
59. Baker JD, Zerner MC (1990) J Phys Chem 94:2866
60. Edwards WD, Zerner MC (1987) Theor Chim Acta 72:347
61. Weissbluth M (1978) Atoms and molecules. Academic Press, New York
62. Rose ME (1957) Elementary theory of angular momentum. Wiley, New York
63. Lefebvre-Brion H, Field RW (1986) Perturbations in the spectra of diatomic molecules. Academic Press, New York
64. Szabo A, Ostlund NS (1989) Modern quantum chemistry. Introduction to advanced electronic structure theory. McGraw-Hill, New York
65. Bethe HA (1929) Ann Physik 3:133
66. Tinkham M (1964) Group theory and quantum mechanics. McGraw-Hill, New York
67. Pitzer RM, Winter NW (1988) J Phys Chem 92:3061
68. Turro NJ (1978) Modern molecular photochemistry. Benjamin/Cummings, Menlo Park
69. Merer AJ (1989) Ann Rev Phys Chem 40:407
70. Törring T, Zimmerman K, Hoeft J (1988) Chem Phys Lett 151:520
71. Dulick M, Field RW, Beaufils JCl, Schamps J (1981) J Mol Spectrosc 87:278
72. Bernard A, Effantin C (1986) Can J Phys 64:246
73. Kaledin LA, Shenyavskaya EA (1981) J Mol Spectrosc 90:590
74. Rösch N, Knappe P, Dunlap BI, Netzer FP (1988) J Phys C: Solid State Phys 102:441
75. Hautecler S, Rosen B (1959) Bulletin de la Classe des Sciences, Academie Royale de Belgique 45:790
76. Dimitriev YN, Kaledin AL, Shenyavkaya EA, Gurvich LV (1984) Acta Phys Hung 55:467